Pole assignment control design for time–varying time–delay systems using radial basis functions

O. L. R. Albrecht and C. J. Taylor
Engineering Department, Lancaster University, UK
Email: o.albrecht@lancaster.ac.uk, c.taylor@lancaster.ac.uk

***Abstract*—Systems with time-varying time delays present a particularly challenging control problem. They have been observed across a wide array of domains, from hydraulic actuators to insulin delivery control systems. Control systems that address system time-delays, nonlinearities and uncertainty are the subject of much research but, whilst the specific concept of varying time delays is sometimes acknowledged (for example in the control of hydraulic manipulators), this appears to be less widely investigated than some other types of nonlinearity. In part motivated by recent research into internal multi-model control, as similarly applied to systems with unknown time-varying delays, the present work utilises a Gaussian radial basis function to switch between two or more partial controllers. Each partial controller is based on a linear model with a (time-invariant) time delay. The new algorithm is developed and evaluated via simulation using a non-minimal state space (NMSS) framework, with pole assignment as the design criterion. Simulation results suggest that it yields improved performance in comparison to a simpler switching approach and the equivalent linear control system. However, laboratory examples and further research into robustness and stability is required in the next step.**

***Index Terms*—uncertain time delay, time-varying delay, Gaussian radial basis function, non-minimal state space model**

I. Introduction

Time-varying, time delay systems present a challenging control problem [1]. This is particularly so when the observed time delay (also referred to as the dead time or lag), between the control input variable and the controlled output, is itself unknown, stochastic and time-varying. In some scenarios, for example, the time-delay (in seconds) between implementing a change in the applied voltage (in either open or closed-loop) and observing the associated angular velocity response for a hydraulically actuated robotic manipulator, can change over time. Such variations in the delay may be caused by the internal dynamics of the system and other nonlinear characteristics, such as fluid compressibility, varying pressure dynamics, dead-band of the pump, valve flow properties and friction characteristics [2–4]. In the latter case, the complex nature of the time delay variability can appear stochastic (rather than, say, dependant on a measured system state).

More generally, system time delays typically consist of an accumulation of delays, including communication delays [5], calculation delays and other internal system delays. In fact, time-varying time delays have been observed across a wide array of domains, from the hydraulic actuators alluded to above to e.g. insulin delivery control systems [6].

In part motivated by reference [7], who develop internal multimodel controllers for systems with unknown delays, the present work similarly proposes a Gaussian radial basis function based approach, here using the weighting function to switch between two or more partial models with different time delays. The new algorithm is developed and evaluated via simulation using a non-minimal state space (NMSS) framework, with pole assignment as the design criterion [8–11].

The Gaussian radial basis function is part of the set of basis functions and takes the following general form [12],

$$\phi(r) = e^{-r^2} \tag{1}$$

where, for example, $r = \frac{(x-y)}{\theta}$, in which θ is a coefficient. This definition of r provides a representation of the proximity between x and y (e.g. for image processing applications) but other forms are also common. Such functions have been used across a wide range of disciplines (for data interpolation [13], electron-nuclear cusp condition calculations [14], etc.). Most commonly in control, however, Gaussian radial basis functions are used in machine learning, as either activation functions in Artificial Neural Networks (ANNs) or as kernel functions in Support Vector Machines (SVMs) [e.g. 15–17].

The present authors have also found a few examples in the literature of radial basis functions being used in the context of variable time-delay systems. However, these are usually for controllers based on neural networks, in which the basis function is an activation function or weighting term [5–7]. By contrast, the present article exploits the existing NMSS model-based design approach [8–11], adapted here in a novel way so that the input signal is a weighted sum of the partial control inputs for different time delay models. This yields a nonlinear weighted proportional-integral-plus (PIP) control system.

Again, weighting equations span many other applications, such as fracture mechanics [18], image processing [19] and time-frequency representations [20]. In the context of variable time delays, a few controllers do exist that exploit weighting functions. For example, [21] develop an interval type-2 (IT2) stochastic fuzzy neural network, where membership functions and weighting functions are used to handle parameter uncertainties, while [22] introduces a robust H-∞ controller, with switching functions and local fuzzy weighting functions. The present work also uses switching control laws, although

This work is supported by the UK Engineering and Physical Sciences Research Council (EPSRC) grant EP/R02572X/1.

here these are obtained via the proposed weighting matrix scheme for NMSS models, with the control system solved via straightforward pole assignment. Section II defines the model and briefly reviews the underlying control design methodology, while section III describes new weighting function approach. This is followed in sections IV and V by a simulation example and conclusions, respectively.

II. Background

The plant is represented as a Transfer function (TF) model, albeit with a time-varying, time delay element, as follows,

$$y(k) = \frac{B(z^{-1})}{A(z^{-1})} u(k - \tau(k) + 1) \tag{2}$$

where $y(k)$ is the output, $u(k)$ is the control input and $\tau(k)$ is the time delay at sample k. Here, $B(z^{-1}) = b_1 z^{-1} + ... + b_m z^{-m}$ and $A(z^{-1}) = 1 + a_1 z^{-1} + ... + a_n z^{-n}$, in which z^{-1} is the backward shift operator, i.e. $z^{-1}y(k) = y(k-1)$.

For control system design, it will be assumed that $\tau(k)$ is known at sample k. Of course, in general, $\tau(k)$ is unknown and must be estimated using one of the methods from the literature, such as the multi-model approach of [7], an on-line version of the first author's recently proposed polynomial-based approach [23], or e.g. [24, 25]. The focus below is to develop a control methodology for the plant model (2), although the robustness to time delay modelling errors is nonetheless investigated via the simulation study (section IV).

Consider a set of N_p control models,

$$y_i(k) = \frac{B_i(z^{-1}) z^{-\tau_i + 1}}{A_i(z^{-1})} u_i(k) \tag{3}$$

where $i = 1 \ldots N_p$, $B_i(z^{-1}) = b_{i,1} z^{-1} + \ldots + b_{i,m_i} z^{-m_i}$, $A_i(z^{-1}) = 1 + a_{i,1} z^{-1} + \ldots + a_{i,n_i} z^{-n_i}$ and τ_i is the time-invariant time delay of the i-th model. In general, analytical or system identification methods can be used to help determine a suitable number of models and their time delays. For the later simulation example, $N_p = 3$ is chosen, with $\tau_1 = 6$, $\tau_2 = 16$ and $\tau_3 = 26$, since this spans the known range of time delays for the problem under study, and yields promising results following initial trial and error experimentation.

Each model (3) is represented in NMSS form and linear PIP control system design proceeds in the usual manner. Page constraints preclude full discussion of the NMSS/PIP approach here; see [8–11] and the numerous references therein. For the model (3), the non-minimal state vector $\mathbf{x}_i(k)$ consists of $y_i(k)$, $y_i(k-1)$, ..., $y_i(k-n_i+1)$, $u_i(k-1)$, ..., $u_i(k-m_i-\tau_i+2)$ and $q_i(k)$, where $q_i(k) = q_i(k-1) + y_d(k) - y_i(k)$, which is the integral–of–error state associated with the i-th model, introduced to ensure type 1 servomechanism performance i.e. steady state tracking of the set point $y_d(k)$.

The NMSS/PIP framework has been chosen here since it facilitates straightforward pole assignment design for (normally time-invariant) time delay systems. The designer selects $n_i + m_i + \tau_i - 1$ closed-loop poles p_i (see example below) and equates these to the closed-loop characteristic equation. The second author's CAPTAIN Toolbox can be used to solve such design problems in MATLAB [26]. Subsequently, the control algorithm is most obviously implemented in conventional state variable feedback form,

$$u_i(k) = -\mathbf{k}_i \mathbf{x}_i(k) \tag{4}$$

where $\mathbf{x}_i(k)$ is the non-minimal state vector, $\mathbf{k}_i$ consists of the $n_i + m_i + \tau_i - 1$ control gains, and $u_i(k)$ is the control input associated with the i-th model. In practice, the above algorithm is usually converted into one of several common implementation structures, for example an incremental form to avoid integral wind-up problems [10].

III. Weighted Controller

The nonlinear weighted PIP controller is designed for the plant (2), where the variable time delay in seconds is represented in discrete time as an integer number of samples, $\tau(k)$. The controller consists of a set of N_p partial controllers, based on the partial models (3), whose control inputs $u_i(k)$ $(i = 1, \ldots, N_p)$ are combined in a weighted sum to determine the composite input $u(k)$ for application to the plant.

For a plant with a known range of time delays, from τ_{min} to τ_{max} samples, N_p is chosen so that each partial controller provides a stable response for a suitable part of this range. Most obviously, the partial models are obtained so that the associated time delays $\tau_1, \tau_2, \ldots, \tau_{N_p}$ are equally spaced in the range τ_{min} to τ_{max}. These values will be referred to as the 'centres' of the partial models and controllers.

The weighted control algorithm is,

$$u(k) = \sum_{i=1}^{N_p} \mu_i(w(k)) u_i(k) \tag{5}$$

where $u(k)$ is the control input, expressed as a weighted sum of the control inputs $u_i(k)$ associated with each partial model, and $\mu_i(w(k))$ is the following weighting function variable,

$$\mu_i(w(k)) = \frac{N_i(w(k))}{D(w(k))} \tag{6}$$

in which,

$$N_i(w(k)) = \exp\left(\frac{-(w(k) - \tau_i)^2}{\sigma_d^2}\right) \tag{7}$$

and,

$$D(w(k)) = \sum_{i=1}^{N_p} \exp\left(\frac{-(w(k) - \tau_i)^2}{\sigma_d^2}\right) \tag{8}$$

where τ_i are user-defined values that represent the centres of the partial controller operating ranges, $\sigma_d \geq 1$ is a dispersion value (a user selected coefficient) and $w(k)$ is the decision variable. Here, $w(k)$ represents the latest estimate of the time delay. In the ideal case, as initially assumed below, the decision variable $w(k) = \tau(k)$.

In equations (7) and (8), $-(w(k) - \tau_i)^2$ determines the distance of $w(k)$ from the centres of the partial controllers. This enables the control input of the controller with the centre closest to $w(k)$ to have the highest weighting. In equation (6),

the weighting value is calculated as a percentage of the whole, ensuring that $0 \leq \mu_i(w(k)) \leq 1$ and $\sum_{i=1}^{N_p} \mu_i(w(k)) = 1$.

For example, if $\tau_{min} = 1$, $\tau_{max} = 31$ and $N_p = 3$, as in the later simulation example, τ_1, τ_2 and τ_3 can be chosen as 6, 16 and 26, respectively. In practice, this choice will depend on the system under study and the chosen sampling rate. Fig. 1 shows how the weighting function values (y-axis of each subplot) determine the relative input from each controller, for time delays $w(k)$ in the range $1 \rightarrow 31$ (x-axis). The upper leftmost subplot of Fig. 1 shows the case when the dispersion variable is set to unity. When $\sigma_d = 1$, for almost all values of $w(k)$, the control effort will come entirely from the partial controller based on the model that is closest to this time delay decision variable; the exceptions are that for $w(k) = 11$ and $w(k) = 21$ (the mid points between τ_1, τ_2 and τ_3), equation (5) becomes $u(k) = (u_1(k) + u_2(k))/2$ and $u(k) = (u_2(k) + u_3(k))/2$ respectively, i.e. a 50–50 split between the two closest controllers.

As shown by the other subplots of Fig. 1, increasing the value of the dispersion coefficient σ_d results in a flattening of the functions, presaging a smoother transition between the partial controllers as the time delay evolves. For $\sigma_d \approx 5 \rightarrow 10$, the weighting function has three clear peaks, each associated with the partial model closest to the current time delay, but with contributions from the other models. For sufficiently large σ_d, equation (5) becomes $u(k) = (u_1(k) + u_2(k) + u_3(k))/3$ and the three partial controllers contribute equally, something that is unlikely to be useful in practice.

IV. Simulations

The preliminary simulation results described here are for a first order model with long time delays, analogous to some of the hydraulic manipulator control models developed by [2–4] i.e. the plant (2) with $n = m = 1$, $a_1 = -0.9$, $b_1 = 1.2$ and $\tau(k)$ represented by a pseudo-Random Walk (RW) in the range $\tau_{min} = 1$ to $\tau_{max} = 31$ samples. As already alluded to above, three partial models have been chosen, each based on the same plant coefficients but with $\tau_1 = 6$, $\tau_2 = 16$ and $\tau_3 = 26$, i.e.,

$$y_i(k) = \frac{1.2z^{-\tau_i}}{1 - 0.9z^{-1}} u_i(k) \tag{9}$$

The non-minimal state vector for each model is,

$$\mathbf{x}(k) = [y_i(k), u_i(k-1), \ldots, u_i(k-\tau_i+1), q_i(k)] \tag{10}$$

and the closed-loop poles are denoted $p_1, p_2, \ldots, p_{1+\tau_i}$.

Following some trial and error experimentation via simulation, a Smith Predictor forward path form [8] of NMSS/PIP control is selected. The authors are also investigating other implementation forms, which may have advantages in practice and this will be reported in future articles. For this model structure, the Smith Predictor is straightforwardly obtained within the NMSS/PIP framework by choosing p_1 and p_2 freely (within the unit circle of the complex z-plane) and the remaining $\tau - 1$ poles to the origin [8, 10]. The results below are based on $p_1 = p_2 = 0.6$, obtained by trial and error simulation to obtain a realistic speed of response in the context of a robotic manipulator.

Guidance on how to chose the dispersion coefficient is being developed by the authors, with $\sigma_d = 5$ used for illustrative purposes here (again selected following some initial trial and error adjustments).

In addition to the new weighted controller, two baseline controllers are developed, as follows,

- Linear PIP control based on the model (9) with $\tau = 16$.
- Basic switching control, in which PIP controllers are designed for each partial model (9), and the time delay is used to select the controller at each sample k, i.e. a simple scheduling controller without a weighting function.

The response of the linear and basic switching controllers, when these are applied to the nonlinear plant (2), are shown in Fig. 2. As might be expected, given the substantial time delay variation illustrated by the lower subplot of Fig. 2, the linear controller yields a highly oscillatory response for much of the simulation. However, when the time delay is comparatively close to the design operating condition for this linear controller, the system is nonetheless stabilised and well controlled for a time. This is a testament to the relative robustness of the Smith Predictor forward path NMSS/PIP approach, even in the simplest linear case [8, 10]. By contrast, the response of the switching controller is satisfactory throughout the simulation experiment.

Fig. 3 and Fig. 4, for sine and square wave set point signals, respectively, highlight the potential improvements obtained using the new weighted algorithm, in comparison to the basic switching approach. The simulation scenario is the same as for Fig. 2, but Fig. 3 is zoomed in to focus on the part of the response were the two approaches most differ. Also, in this case, rather than plotting the sine wave set point, the red trace (upper subplot) shows the theoretical designed-for response of the pole assignment system. The latter is obtained by simulating a TF with the chosen design poles, and a steady state gain of unity, in open loop. Hence, it represents the damping, speed of response etc. that the controller systems designer has chosen via the pole assignment method.

It is clear that the proposed weighted controller more closely follows the ideal response than the basic switching algorithm. This result is quantitatively illustrated in Table I, which shows both the control input variance and the Mean Absolute Error (MAE) between the output and ideal response, for both set point scenarios (in both cases, over all 2000 samples of the simulation experiment, cf. Fig. 2). Table I shows a significant improvement when using the weighted approach, for no additional cost in control actuator activity.

Finally, Fig. 5 and the last two rows of Table I illustrate the relative robustness of the switching and weighted controllers to modelling errors, i.e. when there are substantial differences between the plant time delay and the time delay utilised by the control algorithms. This simulation represents time delay estimation errors, simulated here by using different pseudo-random walk signals for $w(k)$ and $\tau(k)$ (lower subplot of Fig. 5). Although both the basic switching and weighted

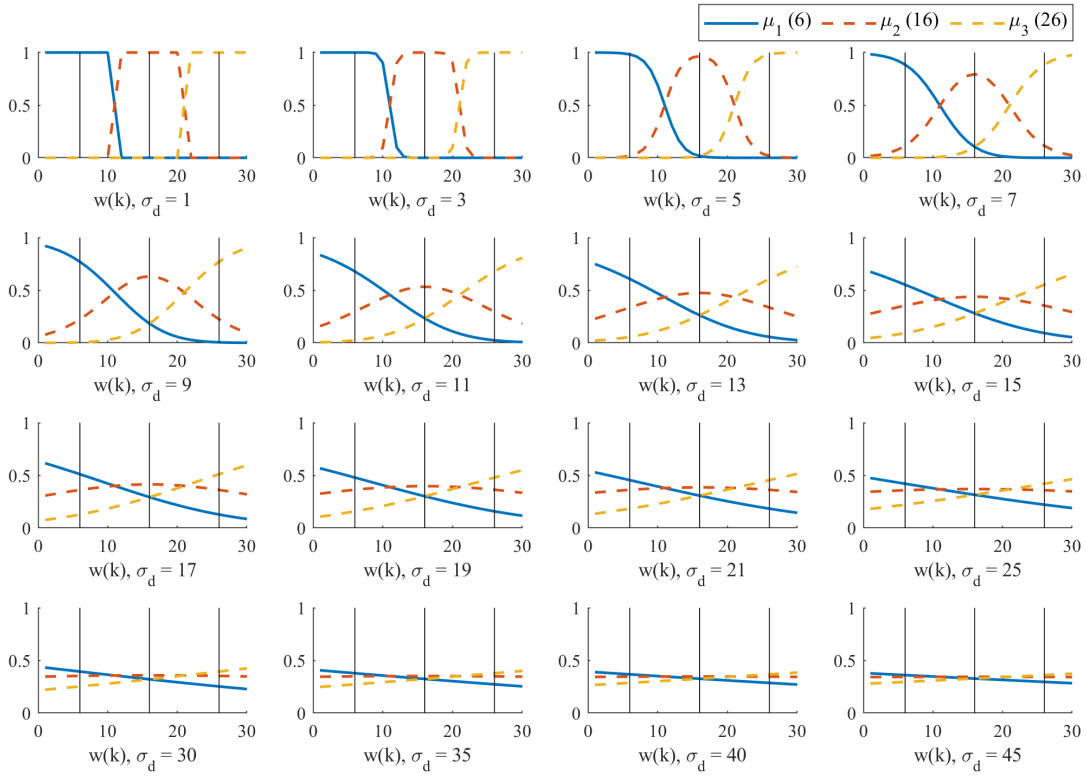

Fig. 1. Graphs showing how weighting values generated by equation (6) depend on the user selected dispersion coefficient σ_d. Each subplot shows $\mu_1(w(k))$ (blue), $\mu_2(w(k))$ (red) and $\mu_3(w(k))$ (orange) (associated with $\tau = 6$, $\tau = 16$ and $\tau = 26$, respectively), plotted against the time delay decision variable $w(k)$. The black, vertical lines mark the centres of the partial controllers.

TABLE I
MEAN ABSOLUTE ERROR BETWEEN THE OUTPUT AND THE IDEAL RESPONSE, AND THE VARIANCE OF THE CONTROL INPUT.

Experiment & Controller	MAE	$var(u)$
Sine wave set point		
Linear control	4.9e3	2.9e7
Basic switching	1.12	0.53
Weighted switching	0.62	0.50
Square wave set point		
Linear control	2.5e3	7.4e6
Basic switching	0.84	0.33
Weighted switching	0.48	0.27
Time delay model mismatch		
Basic switching	2.02	0.45
Weighted switching	1.22	0.49

approaches maintain control throughout the experiment, for some periods of time the new approach yields improved results, hence the reduced MAEs shown in Table I.

Naturally, general conclusions cannot be drawn from these isolated simulations, but the on-going simulation and experimental study being conducted by the authors presages the likely value of the new weighted PIP approach.

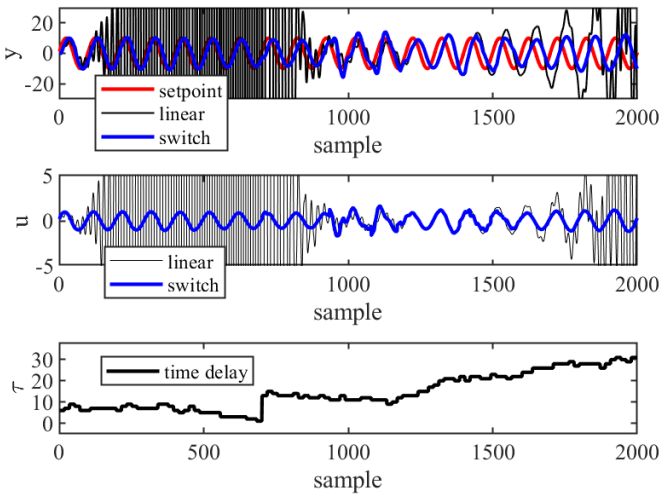

Fig. 2. Comparison of the basic switching control system (without a weighting term) and linear control, showing the set point and outputs (upper subplot), control inputs (middle) and time delay (lower). The simulation uses the first order model $a_1 = -0.9$ and $b_1 = 1.2$, with $\tau_1 = 6$, $\tau_2 = 16$ and $\tau_3 = 26$ samples for the time delays of the switching controller. The linear controller is based on $\tau_2 = 16$, the midpoint of the time delay range in this simulation.

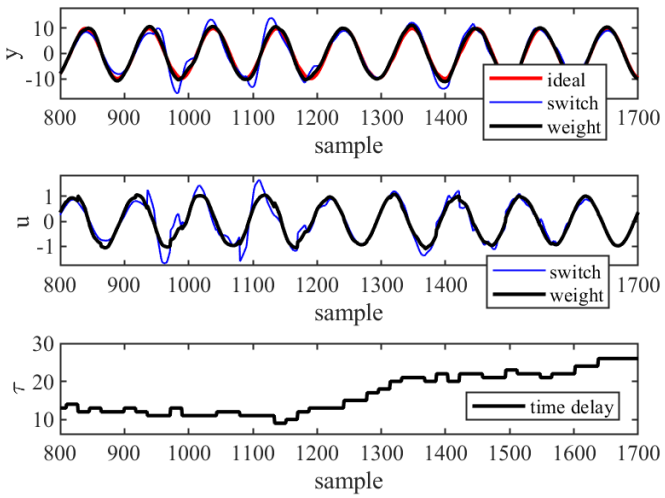

Fig. 3. Comparison of the basic switching and weighted controllers, showing the outputs (upper subplot), control inputs (middle) and time delay (lower). Based on the same simulation experiment as for Fig. 2 but shows the new weighted controller, and is zoomed in to selected sample numbers. Also, instead of the set point, the ideal response (based on the design poles) is shown as a red trace but is largely obscured by the weighted controller (black trace) that closely follows it.

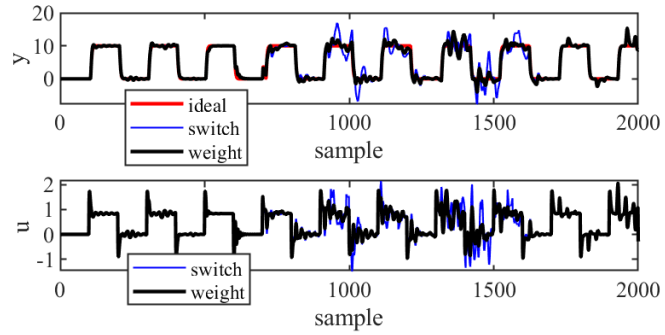

Fig. 4. Comparison of the basic switching and weighted controllers for a square wave set point, showing the ideal response and outputs (upper subplot) and control inputs (lower). The time delay is the same as for Fig. 2.

V. Conclusions

This article has considered the control of discrete-time models with time-varying, sampled time delays. The controller consists of a set of partial controllers, each based on the partial models chosen or estimated by the designer. The control inputs are combined in a weighted sum, based on Gaussian radial basis functions, to determine the control signal for application to the plant. The new algorithm has been developed and implemented using an NMSS framework, with linear PIP pole assignment as the design criterion.

Simulation results suggest that the weighted approach yields improved performance, including less chance of instability,

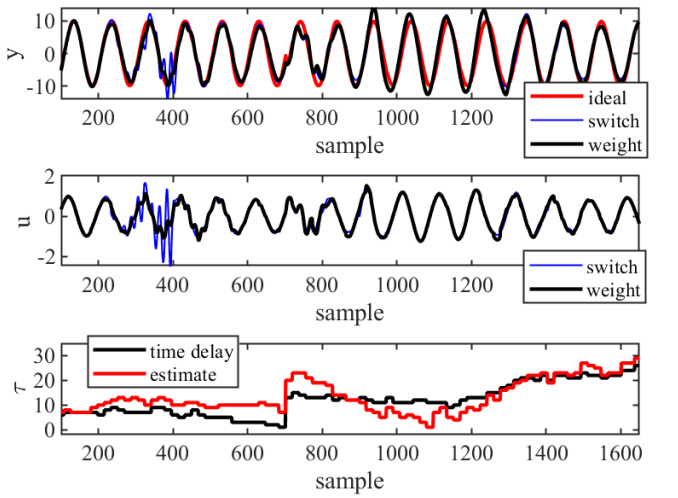

Fig. 5. Comparison of the basic switching and weighted controllers when there are time delay model mismatch errors, showing the outputs (upper subplot), control inputs (middle) and time delays (lower). The 'estimated' time delay has been artificially created using a pseudo-random walk signal, so as to represent an example of time delay modelling errors.

and sometimes better set point tracking and smoother input signals, in comparison to a simpler switching approach and the equivalent linear control systems. Furthermore, the weighted approach more closely follows the theoretical or ideal response, as set by the designer via the closed-loop poles.

However, the proposed approach does require use of a suitable on-line time delay estimation algorithm [24, 25]. Our recent review [2] discusses some of the issues arising in this context. Fortunately, preliminary simulations with time delay modelling errors, suggest that the proposed controller might be relatively robust to realistic scenarios when the time delay is uncertain. However, an analysis of higher order systems, laboratory examples and further research into robustness and stability is required in the next step of this research. Furthermore, the present article assumes the discrete-time plant has an integer number of samples time delay. In future work, continuous-time models will be utilised for the simulation study, so that inter-sampling delays can also be considered.

References

[1] J. E. Normey-Rico and E. F. Camacho. "Dead-time compensators: A survey". In: *Control Engineering Practice* 16.4 (2008), pp. 407–428.

[2] O. L. R. Albrecht and C. J. Taylor. "Unknown and time–varying time delays in the modelling and control of hydraulic actuators: literature review". In: *4th Australian and New Zealand Control Conference (ANZCC)*. Gold Coast, Australia, Nov. 2020.

[3] M. Bandala, C. West, S. Monk, A. Montazeri, and C. J. Taylor. "Vision–based assisted tele–operation of a dual–arm hydraulically actuated robot for pipe cutting and grasping in nuclear environments". In: *Robotics* 8.6: 42 (2019), pp. 1–24.

[4] S. D. Monk, A. Grievson, M. Bandala, C. West, A. Montazeri, and C.J. Taylor. "Implementation and evaluation of a semi-autonomous hydraulic dual manipulator for cutting pipework in radiologically active environments". In: *Robotics* 10.2: 62 (2021), pp. 1–14.

[5] C. I. Aldana, R. Munguía, E. Cruz-Zavala, and E. Nuño. "Pose Consensus of Multiple Robots with Time-Delays Using Neural Networks". In: *Robotica* 37 (2019), pp. 883–905.

[6] Z. Trajanoski and P. Wach. "Neural predictive controller for insulin delivery using the subcutaneous route". In: *IEEE Transactions on Biomedical Engineering* 45.9 (1998), pp. 1122–1134.

[7] S. Ben Atia, A. Messaoud, and R. Ben Abdennour. "An online identification algorithm of unknown time-varying delay and internal multimodel control for discrete nonlinear systems". In: *Mathematical and Computer Modelling of Dynamical Systems* 24.1 (2017), pp. 26–43.

[8] C. J. Taylor, A. Chotai, and P. C. Young. "Proportional–Integral–Plus (PIP) control of time delay systems". In: *IMECHE Proceedings Part I: Journal of Systems and Control Engineering* 212.1 (1998), pp. 37–48.

[9] C. J. Taylor, A. Chotai, and P. C. Young. "Design and Application of PIP controllers: Robust Control of the IFAC93 Benchmark". In: *Institute of Measurement and Control: Transactions* 23.3 (2001), pp. 183–200.

[10] C. J. Taylor, P. C. Young, and A. Chotai. *True Digital Control: Statistical Modelling and Non–Minimal State Space Design*. John Wiley and Sons, 2013.

[11] P. Avery, Q. Clairon, R. Henderson, C. J. Taylor, and E. Wilson. "Robust and adaptive anticoagulant control". In: *The Journal of the Royal Statistical Society, Series C (Applied Statistics)* 69.3 (2020), pp. 503–524.

[12] M. D. Buhmann. "Summary of Methods and Applications". In: *Radial Basis Functions: Theory and Implementations*. Cambridge University Press, 2003. Chap. 2.

[13] R. Yokota, L. A. Barba, and M. G. Knepley. "PetRBF - A parallel O(N) algorithm for radial basis function interpolation with Gaussians". In: *Computer Methods in Applied Mechanics and Engineering* 199.25-28 (2010), pp. 1793–1804.

[14] J. Kussmann and C. Ochsenfeld. "Adding electron-nuclear cusps to Gaussian basis functions for molecular quantum Monte Carlo calculations". In: *Physical Review B - Condensed Matter and Materials Physics* 76.11 (2007).

[15] R. M. Sanner and J.-J. E. Slotine. "Gaussian Networks for Direct Adaptive Control". In: *IEEE Transactions on Neural Networks* 3.6 (1992), pp. 837–863.

[16] Z. R. Yang. "A novel radial basis function neural network for discriminant analysis". In: *IEEE Transactions on Neural Networks* 17.3 (2006), pp. 604–612.

[17] U. Aich and S. Banerjee. "Modeling of EDM responses by support vector machine regression with parameters selected by particle swarm optimization". In: *Applied Mathematical Modelling* 38.11-12 (2014), pp. 2800–2818.

[18] X. C. Zhao, X. R. Wu, and D. H. Tong. "Weight functions and stress intensity factors for pin-loaded single-edge notch bend specimen". In: *Fatigue and Fracture of Engineering Materials and Structures* 38 (2015), pp. 1519–1528.

[19] C. Xu and J. L. Prince. "Generalized gradient vector flow external forces for active contours". In: *Signal Processing* 71 (1998), pp. 131–139.

[20] D. L. Jones and T. W. Parks. "A High Resolution Data-Adaptive Time-Frequency representation". In: *IEEE Transactions on Acoustics, Speech and Signal Processing* 38.12 (1990), pp. 2127–2135.

[21] Y. Pan, Q. Zhou, Q. Lu, and C. Wu. "New dissipativity condition of stochastic fuzzy neural networks with discrete and distributed time-varying delays". In: *Neurocomputing* 162 (2015), pp. 267–272.

[22] Y. Mao and H. Zhang. "Exponential stability and robust H-inf control of a class of discrete-time switched nonlinear systems with time-varying delays via T-S fuzzy model". In: *International Journal of Systems Science* 45.5 (2014), pp. 1112–1127.

[23] O. L. R. Albrecht and C. J. Taylor. "A linear regression variable time delay estimation algorithm for the analysis of hydraulic manipulators". In: *13th UK Automatic Control Council (UKACC) International Conference*. Plymouth, UK, Apr. 2022.

[24] Y. Tan. "Time-varying time-delay estimation for nonlinear systems using neural networks". In: *International Journal of Applied Math and Computer Science* 14.1 (2004), pp. 63–68.

[25] X. M. Ren and A. B. Rad. "Identification of nonlinear systems with unknown time delay based on time-delay neural networks". In: *IEEE Transactions on Neural Networks* 18.5 (2007), pp. 1536–1541.

[26] C. J. Taylor, P. C. Young, W. Tych, and E. D. Wilson. "New developments in the CAPTAIN Toolbox for Matlab with case study examples". In: *18th IFAC Symposium on System Identification (SYSID)*. Stockholm, Sweden, July 2018.